# Evaluation of Four Commercially Produced Surface Treatments

*J.R. Diebel, K. Sridharan, and S.J. Bull*

*(Submitted 30 October 2000)*

**The paper reports the results of characterization of four commercial surface treatments on M2 tool steel substrates. The treatments characterized were (a) TiN deposited by physical vapor deposition (PVD), (b) TiCN/TiN multilayer also deposited by PVD, (c) diamond-like carbon (DLC) deposited by an ion-assisted technique, and (d) vanadium carbide (VC) produced by a thermal diffusion process. The surface treatments were evaluated for characteristics relevant to their tribological performance, such as thickness, roughness, chemical composition, micro- and nanohardness, coating-substrate adhesion, and wear resistance. In addition, a hardness model developed at the University of Newcastle upon Tyne (United Kingdom) to correct for substrate effects was successfully applied. Nanohardness tests also yielded the elastic modulus values of the surface treatments, while scratch testing used for determining coating-substrate adhesion provided qualitative information on their ductility.**

**Keywords** diamond-like carbon, hardness modeling, ion-assisted deposition, physical vapor deposition, thermal diffusion, vanadium carbide

## 1. Introduction

In recent years, the increasing industrial demand for processes that enhance the tribological performance of tools and components has led to the development of a variety of surface treatments.[1] These surface treatments include overlay coatings such as chemical vapor deposition (CVD) and physical vapor deposition (PVD) as well as those involving the infusion of new atomic species into the surface such as thermal-diffusion and ion implantation. More recently, hybrid techniques, multilayer coatings, and functionally graded surfaces with desired properties have also been developed.[2] The performance of these surface treatments is very specific to their intended application, and their suitability therefore depends on several factors including the temperature during surface treatment, surface roughness, coating-substrate adhesion (in the case of overlay coatings), hardness, and wear resistance. Thus, there appears to be a need for a comparison of commercial surface treatments using standard laboratory tests in order to provide basic information regarding their tribological performance. With this objective, four commercial surface treatments were selected for the present study.

## 2. Experimental

### 2.1 Sample Preparation

M2 steel substrates treated by four commercial surface treatments were procured for the present study.

(1) A DLC coating was produced by an ion beam assisted technique at AEA Technology plc. (Harwell, Oxfordshire, UK). In this process, an evaporated low vapor pressure oil is condensed onto the substrate material and then cracked by a 50 keV nitrogen bucket-type ion source. The temperature throughout deposition is less than 80 °C.[3]

(2) TiN and (3) TiCN/TiN multilayer coatings were deposited by electric arc PVD in an MAV40 unit. Samples are preheated to 200 to 485 °C and the deposition is performed at temperatures ranging from 350 to 500 °C and pressures ranging from 4 to 8 $\mu$bar.[4]

(4) A vanadium carbide (VC) diffusion layer was produced by a thermal diffusion process. This process involves immersing the sample in a high-temperature (1000 °C) bath for several hours.[5]

The DLC and PVD coatings were evaluated in the as-received condition. However, the VC sample exhibited high surface roughness and required polishing to facilitate characterization work.

### 2.2 Layer Characterization

The layer thickness was measured by viewing mounted cross sections under a scanning electron microscope (SEM). Surface roughness, $S_a$, the arithmetic mean of the surface perturbations, was measured with an optical profilometer from an area of 0.3 mm$^2$.

Coating-substrate adhesion was measured using a scratch test. For each sample, four scratches were made with a Rockwell C brale diamond indenter with a 120° cone angle and a 200 $\mu$m radius hemispherical tip. Here, the load was increased linearly (10 N/mm) with the distance from 2 to 60 N. Optical and scanning electron microscopy were used to identify failures along the scratches in order to determine the critical load for coating detachment.[6]

Microhardness was measured with the Vicker's hardness test at five loads (50, 100, 200, 300, and 500 gf). Nanohardness measurements were made with a Nanoindenter II (Nano Instruments, Knoxville, TN) at five loads (5, 10, 50, 100, and 500 mN). Nanoindenter measurements also provided information on the Young's modulus of the surface layers. Nanohardness

**J.R. Diebel** and **K. Sridharan,** University of Wisconsin-Madison, Madison, WI 53706. Contact e-mail: diebelj@cae.wisc.edu. **S.J. Bull,** Department of Mechanical, Materials and Manufacturing Engineering, University of Newcastle, Newcastle upon Tyne, NE17RU, United Kingdom. Contact e-mail: jrdiebel@students.wisc.edu.

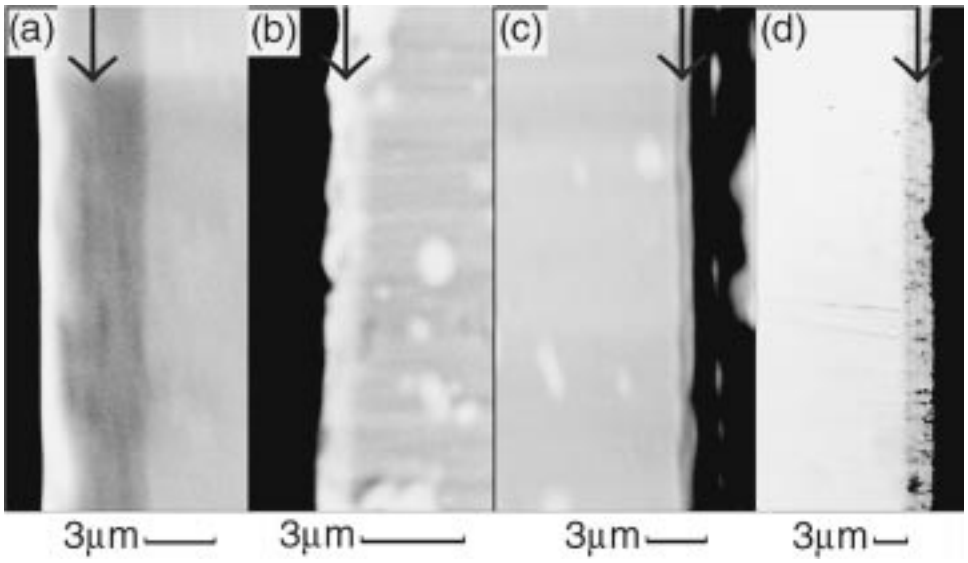


**Fig. 1** SEM micrographs of (**a**) VC, (**b**) DLC, and (**c**) TiN coatings, and an optical photomicrograph of (**d**) TiCN/TiN coating in cross section

**Table 1 A summary of results of characterization of four commercial coatings**

| Layer | | DLC | TiN | TiCN/TiN | VC |
|---|---|---|---|---|---|
| Thickness | | 1.2 $\mu$m | 1.2 $\mu$m | 3.3 $\mu$m | 3.8 $\mu$m |
| Surface roughness $S_a$ | | 7.9 nm | 40 nm | 70 nm | 31 nm(a) |
| Chemical composition | | 94% C, 1.5% O, 4.5% N | 5% C, 4.4% O, 90.6% TiN(b) | Fig. 2 | Fig. 2 |
| Surface adhesion (scratch test) | Failure mode | Exposed substrate at scratch edge | Sharp increase in SEM backscatter image brightness | Edge chips (compressive spallation) | Edge chips (recovery spallation) |
| | Critical load $L_c$ | 21.8 N | 33.7 N | 26.6 N | 15.1 N |
| | Ductility | 2 | 1 (most ductile) | 3 | 4 (least ductile) |
| Coating Hardness | | 13.3 GPa | 16.9 GPa | 41.6 GPa | 34.5 GPa |
| Young's Modulus | | 240.9 GPa | 313.7 GPa | 771.7 GPa | 599.4 GPa |
| Wear rate | | 25,300 $\mu m^3$/m | 27,200 $\mu m^3$/m | 17,100 $\mu m^3$/m | 2620 $\mu m^3$/m |

(a) Polished VC
(b) See Section 3.2

and elastic modulus measurements were extracted from the nanoindentation data by the method of Oliver and Pharr.[7]

A pin-on-disc wear tester was used to characterize the wear performance of the surface treatments. The pin velocity was maintained at 0.1 m/s and an applied load of 2.5 N was used. The pin was a spherical synthetic sapphire, 3 mm in diameter. Under these conditions, the Hertzian contact stress is initially 1 GPa; the contact stress decreases as the wear test progresses. No lubrication was used. The pin-on-disc wear tester also provided information on friction during the progress of the wear test.

## 3. Results and Discussion

### 3.1 General Observation of Layers Viewed in Cross Section

Layer thickness ranges were provided by the suppliers. However, because of the importance of layer thickness in determining the tribological performance of surface treatments, it was decided to obtain more accurate measurements. Figure 1 shows SEM micrographs (a) to (c) and an optical photomicrograph (d) of the layers in cross section. The TiN and DLC samples were of nearly equal thickness (1.2 $\mu$m), but were thinner than the VC and TiCN/TiN multilayers (3.8 and 3.3 $\mu$m, respectively). The TiCN/TiN multilayer coating consisted of six alternating layers of TiCN and TiN; the surface was TiCN. None of the coatings exhibited any delamination from the substrate as a result of metallographic grinding and polishing. The coating-substrate interface appeared more discrete in the PVD TiCN/TiN multilayer and TiN coatings than in the VC and DLC samples, which exhibited a more gradual interface. This is expected since the VC coating was produced by a thermal diffusion process and the DLC coating synthesis involved energetic ion mixing at the coating-substrate interface.

### 3.2 Auger Analysis

The chemical composition of the surface treatments was obtained using scanning Auger electron spectroscopy (AES).

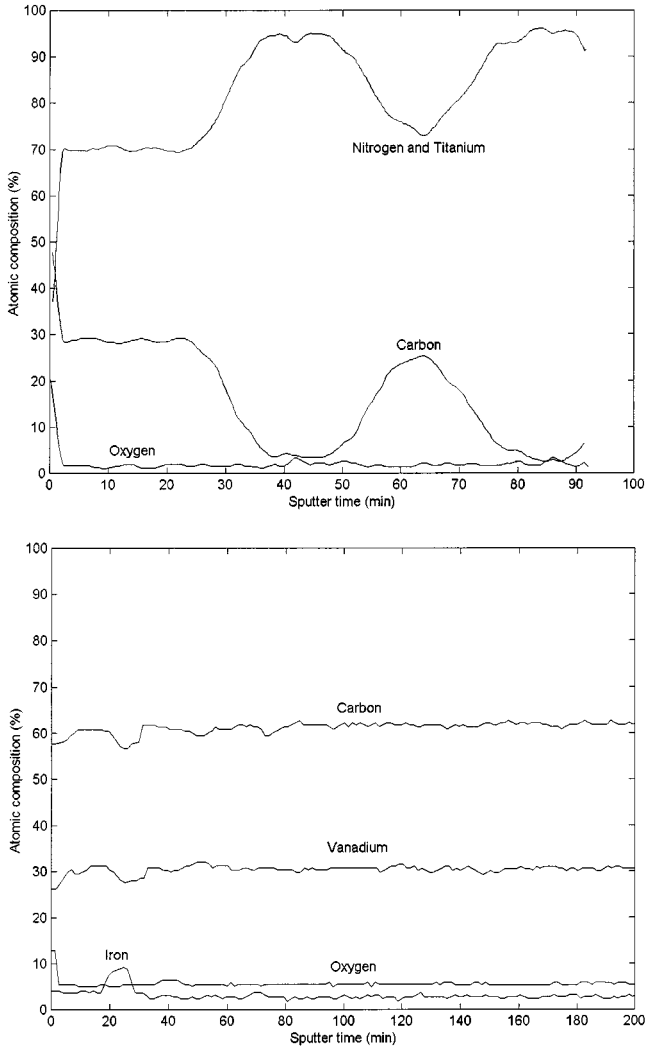


**Fig. 2** Auger depth profiles of TiCN/TiN multilayer (top) and VC (bottom). The individual concentrations of titanium and nitrogen (top) could not be resolved due to the overlap in their Auger transitions (see Section 3.2)

Auger spectroscopy was performed on the surface of the coatings with incremental sputtering occurring perpendicular to the coating-substrate interface. Chemical composition of the TiN and DLC coatings was found not to vary with depth and is reported in Table 1. Chemical composition of the TiCN/TiN multilayer and the VC are plotted against sputter time (which is proportional to depth) in Fig. 2. Neither composition analysis was carried out all the way to the coating-substrate interface. It was noted in the TiCN/TiN multilayer and TiN coatings that an overlap in the nitrogen $KL_{23}L_{23}$ and the titanium $L_3M_{23}M_{23}$ Auger transitions results in a single combined peak at 385 eV. Several algorithms for correcting this overlap have been proposed and this problem remains a topic of research and discussion.[12–15] For this reason, it was chosen to leave the data in raw (uncorrected) form.

### 3.3 Surface Roughness

Surface roughness has a significant effect on the tribological properties of surfaces (wear debris generation, lubrication retention, and friction). The DLC, TiN, and TiCN/TiN were found to have surface roughnesses (RMS) of 10, 40, and 70 nm, respectively. As mentioned earlier, the VC layer was polished prior to evaluation to a roughness of 40 nm. Based on descriptions of PVD-produced TiN in Ref 8, it is speculated that the high surface roughness of the TiN and TiCN/TiN multilayer can be attributed, in part, to the presence of evaporation macroparticles of titanium ejected by the arc evaporation process during deposition.

### 3.4 Coating-Substrate Adhesion and Coating Ductility

No significant cracking or spallation was observed along the scratches in the TiN coating. The failure mode was determined by SEM imaging in the backscattered mode where a sharp increase in brightness was observed at roughly equal loads along all four scratches (Fig. 3a). X-ray spectra (Fig. 3b) revealed that the brighter areas in the backscattered image contained much larger amounts of substrate elements, indicating that coating delamination had occurred at this load.

The same failure mode could not be used for the TiCN/TiN multilayer, because no sharp increases in brightness were observed along the scratches in the SEM backscattered image. Edge chips, however, were observed along all four scratches at roughly equal loads (Fig. 3c). This type of edge chip formation is indicative of compressive spallation;[9] however, it is not clear if the chips formed due to delamination of the interfaces between the individual layers in the multilayer or at the coating-substrate interface.

A few edge chips were found along the scratches in the DLC coating, but their appearance was irregular and is thus best attributed to localized defects in the layer and not to failures at the coating-substrate interface. The SEM backscattered image also did not indicate any clear critical load. The failure mode was defined as the appearance of substrate material at the scratch edge due to plastic deformation of the substrate (Fig. 3e).

The VC layer has no clear interface with the substrate since it is diffused, not deposited. Edge chips, however, were observed at roughly equal loads along all four scratches. These edge chips (Fig. 3d), identified as recovery spallation,[9] are indicative of a failure in the interfacial region of the layer and were defined as the critical load. Critical loads and failure modes are reported in Table 1.

Since several different failure modes were used to find critical loads, it is important to include mention of the failure mode observed when citing the critical load. This also shows that critical loads for different coatings are often not directly comparable. However, the type of failure mode exhibited can also be used to characterize the coating's ductility,[9] which is particularly important since traditional methods for determining ductility do not apply well to surface coatings. The presence of a substantially larger number of edge chips in the TiCN/TiN and VC than in the TiN and DLC suggests lower ductility. Similarly, the edge chips on the VC (Fig. 3d) were larger, sparser, and more elongated than the edge chips on the TiCN (Fig. 3c), suggesting that the TiCN/TiN is more ductile. Likewise, the larger number of tensile cracks in the DLC (Fig. 3e) than in the TiN suggests that TiN is more ductile. A qualitative hierarchy of coating ductility, established from these observations, is reported in Table 1.

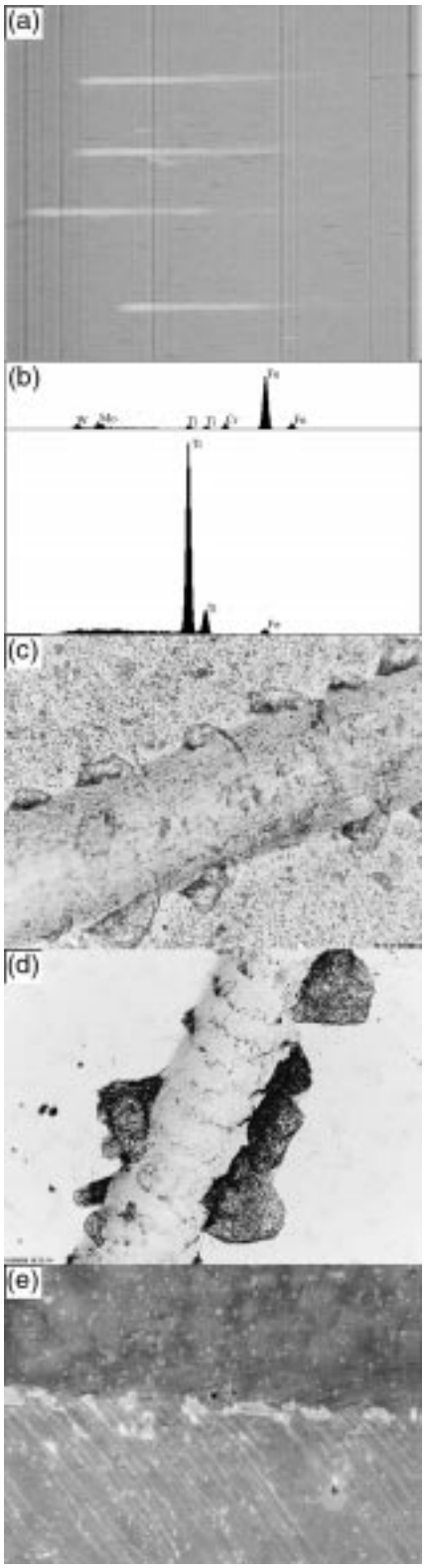


**Fig. 3** Results of imaging studies showing a variety of surface adhesion failure modes: (**a**) SEM backscattered image of scratches in TiN, (**b**) x-ray spectrum of lighter areas (top) and darker areas (bottom) in (**a**), (**c**) compressive spallation at the edge of a scratch in TiCN/TiN, (**d**) recovery spallation at the edge of a scratch in VC, and (**e**) exposed substrate at the edge of a scratch in DLC

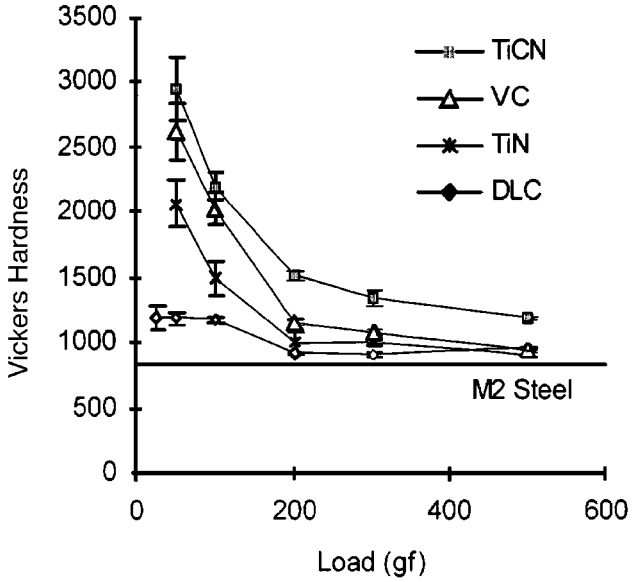


**Fig. 4** Measured microhardness of coating-substrate system as a function of test load

### *3.5 Hardness and Elastic Modulus*

Vickers microhardness as a function of load is shown in Fig. 4. As expected, the measured hardness was found to be load dependent, due to the substrate effect at high loads. As the load was reduced, the indentation depth was reduced and the measured hardness approached the coating hardness. Variation in hardness measurements for a given load also increased as the load was reduced. This increase can be attributed to the increased effect of microscopic surface features on the hardness measurement (as is indicated by the general correlation between surface roughness and the standard devation of hardness measurements at low loads). As the load was increased, the indentation depth was increased and the measured hardness converged on the substrate hardness. Nanohardness results were also found to be load dependent.

The incorporation of substrate effects is a ubiquitous problem in hardness measurements of surface modified materials in general. In order to extract the true hardness of the coating, a model for the hardness of coated systems that has recently been developed at the University of Newcastle upon Tyne (United Kingdom) was applied to the experimental data. This model has been sucessfully tested with the experimental data from a number of coatings.[10] The model fits experimentally obtained hardness (both nano- and microhardness), $H_{measured}$, to the equation

$$H_{measured} = H_{substrate} + \frac{H_{coating} - H_{substrate}}{1 + k\beta^2}$$

where $H_{coating}$ is the coating hardness; $H_{substrate}$ is the substrate hardness; $\beta = \delta/t$ is the experimentally obtained indentation depth, $\delta$, normalized with respect to the coating thickness, $t$; and $k$ is a constant proportional to the coating thickness. Best-fit plots are shown in Fig. 5 and coating hardness is reported in Table 1. The VC and TiCN/TiN multilayer were found to

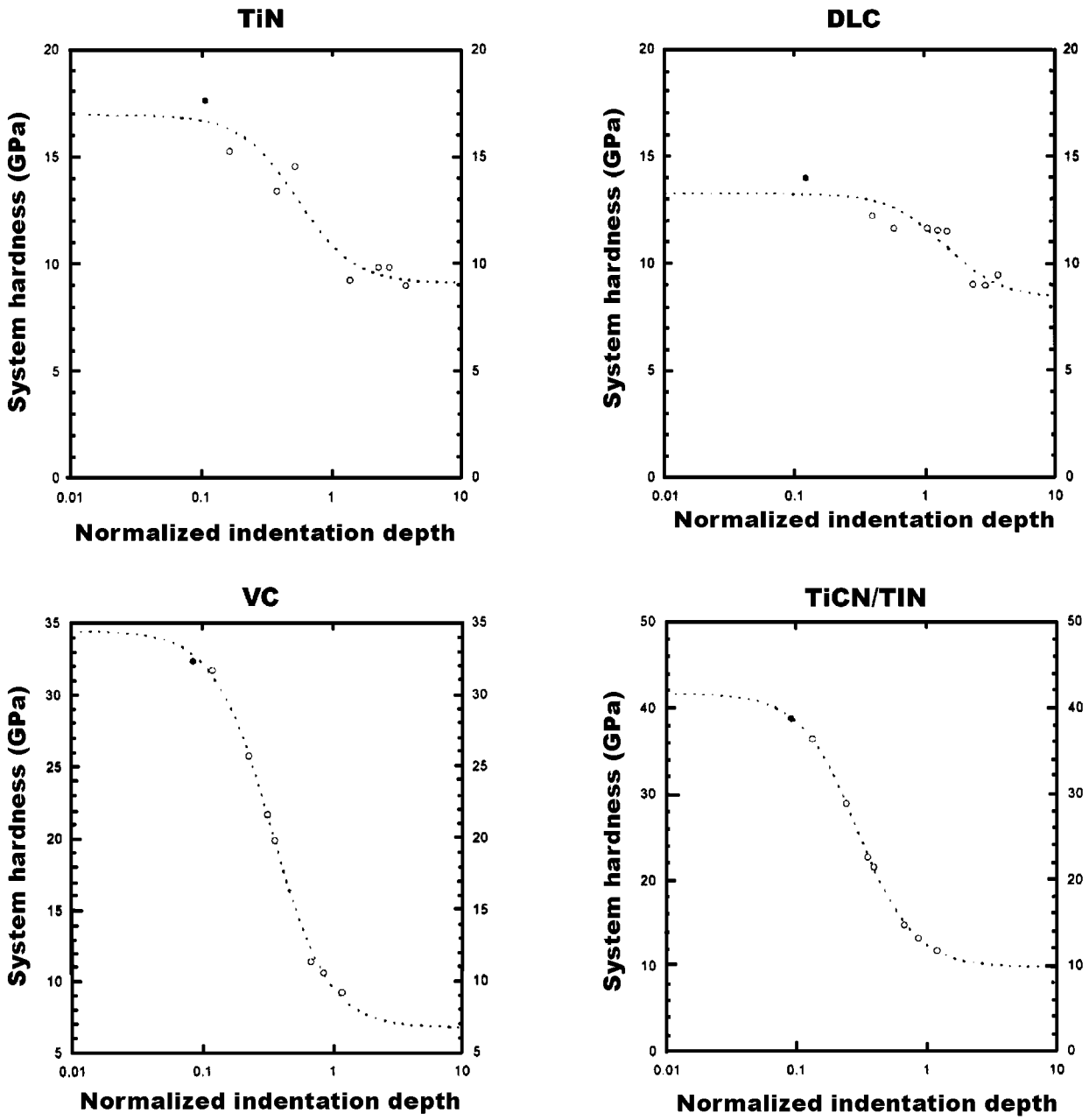


**Fig. 5** Surface hardness results obtained by fitting experimentally obtained values of micro- and nanohardness testing to the model proposed by Korsunsky *et al.*[9]

fit the model best with correlation coefficients ($R$) of 1.0 and 1.0, respectively. The DLC and TiN layers had lower correlation coefficients of 0.93 and 0.96, respectively. The greater variability of the TiN and DLC data results from the larger contribution to the measured hardness made by the substrate, which contains intermittently spaced carbides with very high hardness. Indents made over carbides in thin coatings such as the TiN and DLC have a much larger effect on the measured hardness than in thicker coatings such as the TiCN/TiN and VC.

Nanoindenter elastic modulus data are shown as a function of load in Fig. 6. The elastic modulus was derived from the load versus displacement curve during unloading and was also found to be load dependent. In order to minimize the effect of the substrate, the elastic modulus from the lowest load nanoindentation series (solid circle in Fig. 3) is cited in Table 1. Representative load versus displacement curves were selected from the series from which the elastic moduli were derived and are shown in Fig. 7.

### *3.6 Wear Resistance*

Wear tests were run for 140 min (corresponding to a wear track length of 870 m) or until the substrate was thought to

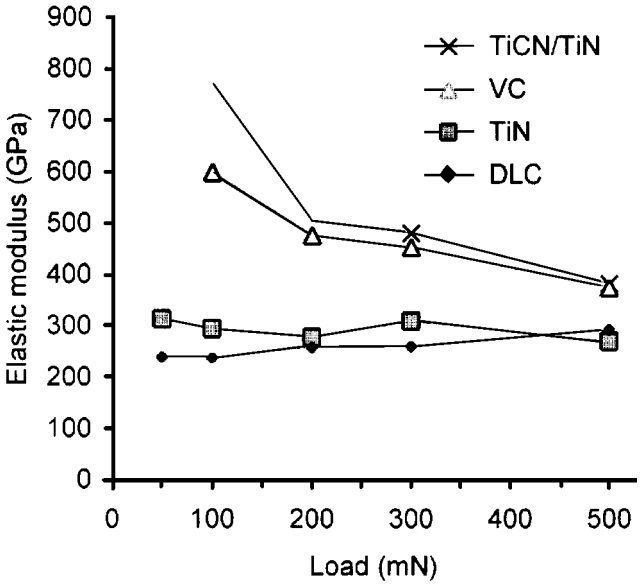


**Fig. 6** Elastic modulus values of the layers (as determined from nanoindenter tests) as a function of test load

be exposed. For DLC, TiN, and TiCN/TiN coated samples, tests were all stopped prematurely (at 187, 348, and 746 m, respectively) upon observation of an increase in acoustic emissions that was thought to be indicative of substrate exposure. Later measurement revealed the substrate was only exposed on the TiN, which had worn to 140% the depth of the coating. The DLC wore to 89% and the TiCN/TiN to 63%. For the case of the VC coating, the wear tests were performed for the entire140 min, after which only 17% of the coating had been worn. The depth of the wear tracks and wear rates were calculated from the widths of the wear tracks and the known indenter geometry using the ASTM G 99 standard[11] and are reported in Fig. 9. Wear rates are also reported in Table 1 and friction versus revolutions plots are shown in Fig. 8.

The high friction observed during the wear test of the DLC coating is due to adhesion between the saphire and the coating. This is compounded throughout the course of the test by the accumulation of wear debris, which is of particular importance as the adhesion between the saphire and coating material prevents the debris from graphitizing to form the low friction layer usually observed when sliding against steel.

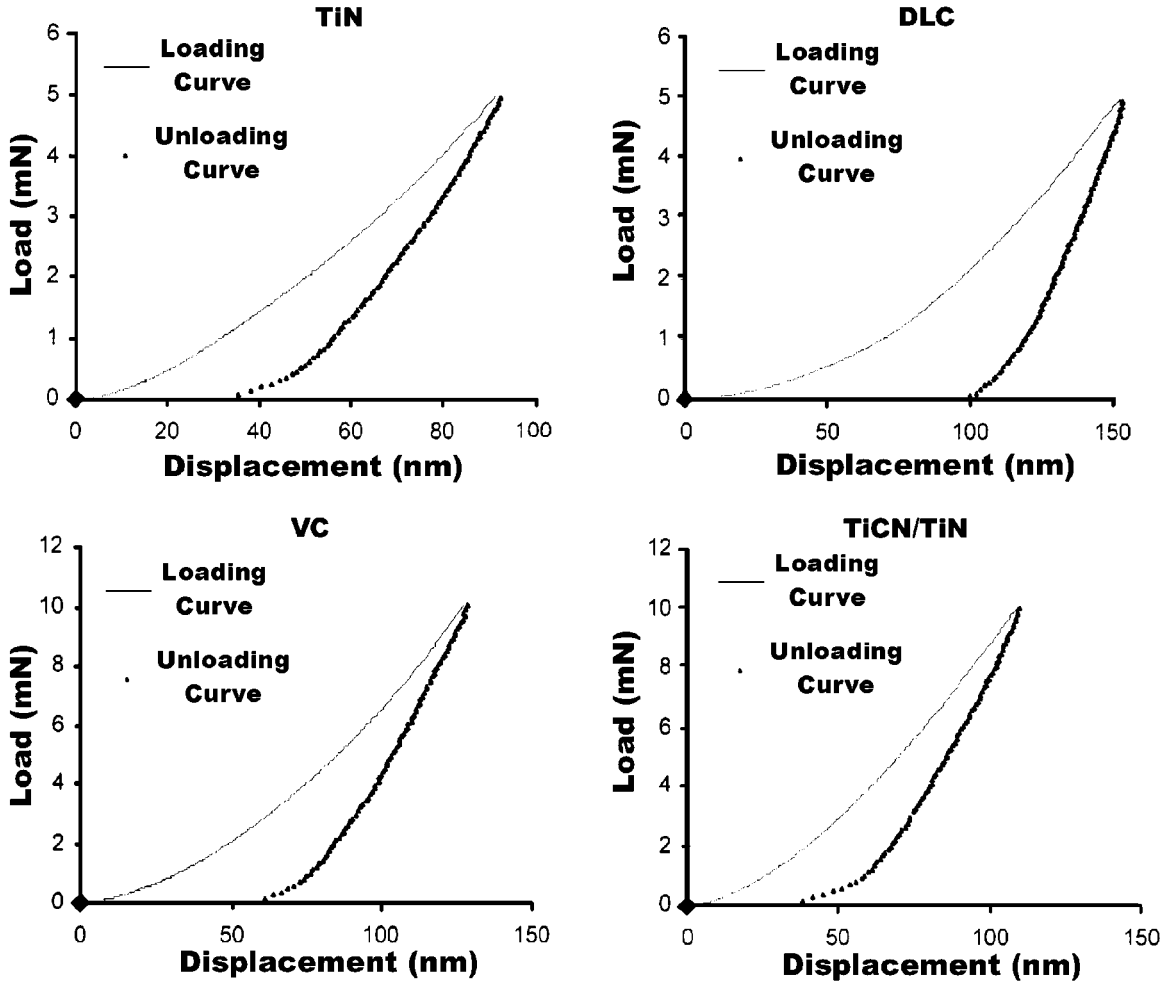


**Fig. 7** Representative nanoindenter load vs displacement plots from the lowest load nanoindentation series (5 mN for TiN, DLC; 10 mN for TiCN/TiN and VC). Elastic modulus data reported in Table 1 were derived from the unloading curves

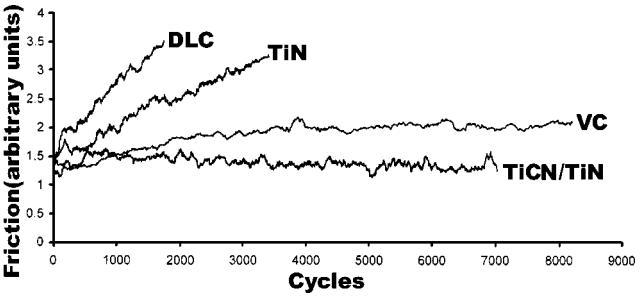


**Fig. 8** Friction vs revolutions plots for the pin-on-disc wear tests (stylus: saphire and nonlubricated)

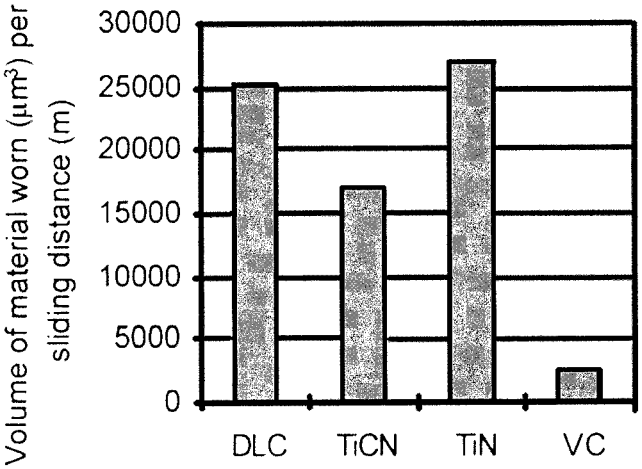


**Fig. 9** Pin-on-disc wear rates for the coatings investigated in this study

## 4. Summary and Conclusions

Two PVD coatings, TiN and multilayered TiCN/TiN, a DLC coating produced by an ion-assisted process, and a VC thermal diffusion coating produced by the thermal diffusion process have been evaluated using a series of laboratory tests. The thicknesses of the DLC and TiN coatings were comparable (1.2 $\mu$m), while the thicknesses of the multilayered TiCN/TiN and thermal diffusion VC coatings were 3.3 and 3.8 $\mu$m, respectively. The DLC coating exhibited the lowest surface roughness by a large margin, followed by the two PVD coatings, TiN and TiCN/TiN. The surface of the VC coating in the as-received condition contained large surface unulations, and, consequently, its surface roughness measurements could not be meaningfully compared to the other three coatings. Scratch tests carried out in conjunction with SEM examination of the scratch edge qualitatively indicated the TiN coating to be the most ductile and adherent to the substrate. The VC and multilayer TiCN/TiN coatings exhibited very high nanohardness values, but the VC coating was the most wear resistant under the test conditions. The results are summarized in Table 1.

### References


1. *ASM Handbook*, vol. 5, *Surface Engineering*, C.M. Cotell, J.A. Sprague, and F.A. Smidt, eds., ASM International, Materials Park, OH, 1994.
2. *Surface Modification Technologies X*, T.S. Sudarshan, K.A. Khor, and M. Jeandin, eds., The Institute of Materials, London, 1997.
3. A.R. McCabe, A.M. Jones, S.J. Bull, and C. Johnston: *Diamond Related Mater.*, 1994, vol. 3 (10), p. 1265.
4. P.A. Dearnley: *Heat Treatments Met.*, 1987, vol. 4, p. 83.
5. R. Arter: *Tooling and Production*, vol. 56, no. 7, pp. 72-74, Oct., 1990.
6. A.J. Perry: *Surf. Eng.*, 1986, vol. 2-3, p. 183.
7. W.C. Oliver and G.M. Pharr: *J. Mater. Res.*, 1992, vol. 7, p. 917.
8. M. Benmalek, P. Gimenez, J.P. Peyre, and C. Tournier: *Surf. Coatings Technol.*, 1991, vol. 48, p. 181.
9. S.J. Bull: *Surf. Coatings Technol.*, 1991, vol. 50, p. 25.
10. A.M. Korsunsky, M.R. McGurk, S.J. Bull, and T.F. Page: *Surf. Coatings Technol.*, 1998, vol. 99, pp. 171-83.
11. *Standard Test Method for Wear Testing with a Pin-on-Disk Apparatus*, G 99, ASTM, Warminster, PA, 1990.
12. A. Chen, J. Firmiss, and J.R. Conrad: *J. Vac. Sci. Technol.*, 1994, vol. B12 (2), p. 918.
13. P.T. Dawson and K.K. Tzatzov: *Surf. Sci.*, 1985, vol. 149, p. 105.
14. A.J. Perry, C. Strandberg, W.D. Sprowl, S. Hoffman, C. Ernsberger, J. Nickerson, and L. Chollet: *Thin Solid Films*, 1987, vol. 169, p. 153.
15. D.G. Watson, W.F. Stickle, and A.C. Diebold: *Thin Solid Films*, 1988, vol. 193, p. 305.